

HYPERMONO: A Monotonicity-aware Approach to Hyper-Relational Knowledge Representation

Zhiwei Hu, Víctor Gutiérrez-Basulto, Zhiliang Xiang, Ru Li, Jeff Z. Pan,

Abstract—In a hyper-relational knowledge graph (HKG), each fact is composed of a main triple associated with attribute-value qualifiers, which express additional factual knowledge. The hyper-relational knowledge graph completion (HKGC) task aims at inferring plausible missing links in a HKG. Most existing approaches to HKGC focus on enhancing the communication between qualifier pairs and main triples, while overlooking two important properties that emerge from the monotonicity of the hyper-relational graphs representation regime. *Stage Reasoning* allows for a two-step reasoning process, facilitating the integration of coarse-grained inference results derived solely from main triples and fine-grained inference results obtained from hyper-relational facts with qualifiers. In the initial stage, coarse-grained results provide an upper bound for correct predictions, which are subsequently refined in the fine-grained step. More generally, *Qualifier Monotonicity* implies that by attaching more qualifier pairs to a main triple, we may only narrow down the answer set, but never enlarge it. This paper proposes the **HYPERMONO** model for hyper-relational knowledge graph completion, which realizes stage reasoning and qualifier monotonicity. To implement qualifier monotonicity HYPERMONO resorts to cone embeddings. Experiments on three real-world datasets with three different scenario conditions demonstrate the strong performance of HYPERMONO when compared to the SoTA.



1 INTRODUCTION

KNOWLEDGE graphs (KGs) store graph-like knowledge as a collection of factual triples [1], [2], [3]. Each triple (h, r, t) in a KG represents a connection between the head entity h and the tail entity t through the relation type r , e.g., $(James\ Harden, member_of_team, Philadelphia\ 76ers)$ in Figure 1. Knowledge graphs provide the backbone of various applications like query answering [4], [5], [6], search [7], [8], entity typing [9], [10] and recommendation systems [11], [12]. In hyper-relational knowledge graphs (HKGs), hyper-relational facts enhance binary relational facts by augmenting triples with supplementary knowledge expressed in the form of attribute-value qualifier pairs $(a : v)$. For example, in Figure 1, the triple $(James\ Harden, member_of_team, Philadelphia\ 76ers)$ is contextualized by the qualifier pairs $\{(start_time: 2019), (end_time: 2023), (teammate: P.J.\ Tucker), (part_of: Atlantic\ Division)\}$, describing teams of the *Atlantic Division* in which *James Harden* and *P.J. Tucker* played together from 2019 to 2023. Like standard KGs, HKGs also suffer from incompleteness. The hyper-relational knowledge graph completion (HKGC) task, which aims at inferring missing links in HKGs, has therefore become an important research topic.

A wide variety of approaches to HKGC have been already proposed, including embedding-based [13], [14],

- Z. Hu and R. Li are with the School of Computer and Information, Shanxi University, Shanxi, China.
E-mail: zhiwei.hu@whu.edu.cn; liru@sxu.edu.cn
- V. Gutiérrez-Basulto and Z. Xiang are with the School of Computer Science and Informatics, Cardiff University, Cardiff, UK.
E-mail: gutierrezbasultov@cardiff.ac.uk; xiangz6@cardiff.ac.uk
- J. Pan is with the school of Informatics, University of Edinburgh, Edinburgh, UK.
E-mail: j.z.pan@ed.ac.uk

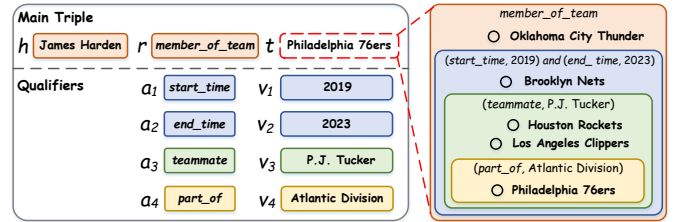


Fig. 1: Qualifier Monotonicity: The box on the right presents all five answers to the query $q = (James\ Harden, member_of_team, ?)$. If qualifiers are added to the query, the number of possible answers is reduced, e.g., if we add the qualifier pairs $(start_time, 2019)$ and $(end_time, 2023)$ to q , *Oklahoma City Thunder* is not a possible answer anymore.

[15], [16], transformer-based with graph neural networks (GNNs) [17], [18] and transformer-based without GNNs methods [19], [20], [21], [22], [23]. Despite the substantial progress achieved so far, each of these approaches has its own disadvantages: embedding-based methods can be categorized into n-ary, key-value pairs and main triple+key-value pairs depending on how facts are defined. While hyper-relational knowledge is effectively represented, the modeling of distinct auxiliary information is done independently. This independence imposes constraints on the interaction between key-value pairs within a given fact. Transformer-based with GNNs methods mainly rely on multi-layer GNNs operations to encode qualifier-pairs information into the main triple, inevitably introducing noise that propagates as the number of GNN layers increases. In addition, the use of GNNs introduces a considerable computational burden. Transformer-based without GNNs methods capture the structure of HKGs within the transformer architecture, thereby avoiding the increase in com-

putational complexity. However, although these methods are in a dominant position on the HKGC task, they overlook two important properties: *Two-Stage Reasoning* and *Qualifier Monotonicity*. When inferring missing entities, two-stage reasoning permits to first reason about binary relational knowledge and then, guided by the results from the previous step, reason about hyper-relational knowledge. Qualifier monotonicity implies that the addition of qualifier information to triples might allow for additional inferences, without invalidating those derived solely from considering main triples. Specifically, these two properties can be described as follow.

- 1) **Two-Stage Reasoning** allows for a two-step reasoning process, facilitating the integration of coarse-grained inference results derived solely from main triples and fine-grained inference results obtained from hyper-relational facts with qualifiers. In the initial stage, coarse-grained results provide an upper bound for correct predictions, which are subsequently refined in the fine-grained step. For example, in Figure 1, the initial stage derives the following coarse-grained answer set from the main triple: $Ans = \{Oklahoma\ City\ Thunder, Houston\ Rockets, Brooklyn\ Nets, Philadelphia\ 76ers, Los\ Angeles\ Clippers\}$. Ans provides an upper bound to be refined in a subsequent step: after adding qualifiers to the main triple, Ans is narrowed down to $\{Philadelphia\ 76ers\} \subseteq Ans$. Hence, in practice, the outcomes of coarse-grained inference can serve to delimit the decision boundaries of fine-grained predictions, mitigating the occurrence of answer drift phenomena.
- 2) **Qualifier Monotonicity** generally implies that for a given hyper-relational query q , as the number of qualifier pairs in q increases, the answer set of q over a HKG might shrink but it never expands, while conversely removing qualifiers from q could only lead to more possible answers. For example, for the query (*James Harden, member_of_team, ?*) in Figure 1, $?$ has five possible answers $\{Oklahoma\ City\ Thunder, Houston\ Rockets, Brooklyn\ Nets, Philadelphia\ 76ers, Los\ Angeles\ Clippers\}$. If the qualifier pairs (*start_time: 2019*) and (*end_time: 2023*) are added, then *Oklahoma City Thunder* is not a possible answer anymore. The main challenge for qualifier monotonicity lies in devising a representation that accurately captures its essence. It should possess the capability to faithfully capture the shrinking-like dynamics induced by the incorporation of qualifiers. In the context of embedding-based methods, ShrinkE [16] has explored qualifier monotonicity through box embeddings. However, the inherent limitations of the embedding-based methods lead to a large gap between ShrinkE’s accuracy and that of SoTA models, as shown in § 5.1, Table 2.

To address the above limitations of existing methods, we introduce a monotonicity-aware framework for hyper-relational knowledge representation (HYPERMONO). To infer the missing tail entity in hyper-relational queries, HYPERMONO first introduces the *Head Neighborhood Encoder* module to encode the content of the neighbors of the head entity. It considers coarse-grained and fine-grained neighborhood aggregators, characterized by the use of either main triples or complete hyper-relational facts to determine

the neighbors of an entity. HYPERMONO further implements two-stage reasoning through a *Missing Entity Predictor* module, which contains two types of predictors: *Triple-based Predictor* and *Qualifier-Monotonicity-aware Predictor*. They differ on whether only main triples or triples+qualifiers are used for prediction. Additionally, HYPERMONO employs cone embeddings to achieve qualifier monotonicity. We utilize cones instead of boxes (as done in ShrinkE) since the main objective is to obtain an answer set qualified by hyper-relational knowledge in a universal subset space. However, the offsets of boxes are unbounded, and how to find boxes to represent a universal set is thus unclear. Cone embeddings naturally represent any finite universal set and its subsets with a proper aperture, as the aperture of cones is bounded from 0 to 2π [4], [6], [24]. Our contributions can be summarized as follows:

- We propose HYPERMONO, a competitive monotonicity-aware model for hyper-relational knowledge graph completion, which simultaneously considers the two-stage reasoning and qualifier monotonicity properties.
- We model each qualifier as a cone space shrink transformation that narrows down the answer set.
- We conduct experiments on three real-world datasets under three different conditions. The obtained results demonstrate the strong performance when compared with SoTA models.

2 RELATED WORK

In this section, we analyze the existing work in the field of HKGC. They can be categorized as follows: Embedding-based Methods (§ 2.1), Transformer-based with GNNs Methods (§ 2.2), Transformer-based without GNNs Methods (§ 2.3), and Other Methods (§ 2.4).

2.1 Embedding-based Methods

Depending on how the facts are represented, embedding-based methods can be classified as n-ary, key-value pairs and main triple+key-value pairs. (i) In n-ary methods, each fact consists of a pre-defined relation r with n corresponding values, denoted as $r(v_1, v_2, \dots, v_n)$. For instance, m-TransH [13] and RAE [14] generalize TransH [25] by projecting all entities onto a relation-specific hyperplane, while m-CP [26] generalizes Canonical Polyadic (CP) decomposition [27], n-Tucker [28] and GETD [28] generalize Tucker [29] to the higher-arity case. However, these methods convert n-ary facts using one abstract relation, ignoring the semantic distinction of different values for each relation. (ii) In key-value pairs methods, each fact is viewed as a set of attribute-value pairs, denoted as $\{(a_i : v_i)\}_{i=1}^m$. For instance, NaLP [15] employs a convolutional neural network followed by a multi-layer perceptron to measure the validity of a fact, RAM [30] further encourages the relatedness among different attributes and between an attribute and all corresponding values. However, these methods treat all attribute-value pairs equally and do not distinguish the main triple from the complete fact. (iii) Main triple+key-value pairs methods regard each fact as a main triple with attribute-value pairs, denoted as $((h, r, t), \{(a_i : v_i)\}_{i=1}^m)$. For example, HINGE [15] and NeuInfer [31] independently

consider each auxiliary pair in the main triple. MSeaKG [32] develops a generic message passing function to encode hyper-relational facts. However, as different auxiliary information is modeled independently, these methods do not properly encode the interactions between attribute-value pairs within fact, further leads to a certain degree of semantic gap between different attribute pairs.

2.2 Transformer-based with GNNs Methods

StarE [17] adopts a message passing based graph encoder CompGCN [33] to obtain the entity and relation embeddings, which are further passed through a transformer decoder to obtain a probability distribution over all entities. QUAD [18] simultaneously takes into account the communication from qualifiers to the main triple and the flow of information from the main triple to qualifiers. It also introduces an auxiliary task to further improve performance. However, these methods primarily employ multi-layer GNNs to incorporate hyper-relational knowledge into the main triple, which inevitably introduces two problems. On the one hand, although multi-layers GNNs operations can encode entity-neighborhood information, they may introduce noise, which can be propagated in a cascading fashion as the number of layers increases. On the other hand, GNNs operations incur in an additional time and space overhead [34], [35], [36], which brings greater challenges to efficiently train these models.

2.3 Transformer-based without GNNs Methods

Many methods abandon the use of GNNs operations and instead incorporate hyper-relational knowledge through various transformer structures. For example, HyTrans [19] extends StarE by substituting the graph encoder with a light-weight relation or entity embeddings. GRAN [20] implements edge-biased fully-connected attention into transformers to encode the graph structure and its heterogeneity. HyNT [21] defines a specialized context transformer to exchange information between the main triple and its qualifiers, HAHE [22] proposes a hierarchical attention structure with global-level and local-level attention to simultaneously model graph-like and sequential content. HyperFormer [23] introduces a mixture-of-experts strategy into the feed-forward layers of a transformer to strengthen its representation capabilities. However, these methods have two shortcomings: on the one hand, they only consider a fine-grained inference steps with hyper-relational knowledge and overlook coarse-grained inferences solely based on the main triples. On the other hand, they do not explicitly embody qualifier monotonicity. We note in passing that although the embedding-based method ShrinkE [16] takes qualifier monotonicity into account, its embedding-based nature results in a large gap in performance when compared with the state-of-the-art, as shown in § 5.1, Table 2.

2.4 Other Methods

Some researchers have tried to introduce external knowledge (e.g., schema information) into the representation of entities and relations to assist HKGC tasks. sHINGE [37] captures not only the primary structural information in

the triples and associated key-value pairs, but also the schema information encoded by entity-typed triples and corresponding entity-typed key-value pairs. DHGE [38] proposes a dual-view hyper-relational structure that contains a hyper-relational instance view for entities and a hyper-relational ontology view for concepts to encode hierarchical knowledge. However, these methods require acquisition of external knowledge relative to the entity, which poses a greater challenge to their general applicability. Considering the fairness of the experimental comparison and that the main goal is the construction of a more general model, we did not consider these baselines.

3 BACKGROUND

In this section, we introduce necessary background on Hyper-relational Knowledge Graphs (§ 3.1), Qualifier Monotonicity (§ 3.2), and Cone Embeddings (§ 3.3).

3.1 Hyper-relational Knowledge Graph

A *hyper-relational knowledge graph* (HKG) \mathcal{G} is defined as $\{\mathcal{E}, \mathcal{R}, \mathcal{H}\}$, where \mathcal{E} is a set of entities, \mathcal{R} is a set of relation types, and $\mathcal{H} = \{(h, r, t, \mathcal{Q}) \mid h \in \mathcal{E}, r \in \mathcal{R}, t \in \mathcal{E}\}$ is a set of *hyper-relational facts*, such that (h, r, t) denotes the *main triple* and $\mathcal{Q} = \{(a_1 : v_1), \dots, (a_n : v_n) \mid a_i \in \mathcal{R}, v_i \in \mathcal{E}\}$ is a set of auxiliary attribute-value *qualifier pairs*. We use $\mathcal{G}_{\text{triple}}$ to denote the set of main triples occurring in \mathcal{G} . Note that when $n = 0$, \mathcal{G} is a standard knowledge graph, i.e., only containing main triples. Under this representation schema, the main triple (*James Harden, member_of_team, Philadelphia 76ers*) in Figure 1 with its qualifiers can be represented as: $\{(James\ Harden: member_of_team, Philadelphia\ 76ers), (start_time: 2019), (end_time: 2023), (teammate: P.J.\ Tucker), (part_of: Atlantic\ Division)\}$. Following the definition of the knowledge graph completion task, the *hyper-relational knowledge graph completion* (HKGC) task on \mathcal{G} looks at predicting a missing entity $?$ in one of the following forms: $(?, r, t, \mathcal{Q})$ or $(h, r, ?, \mathcal{Q})$. Without loss of generality, in what follows we concentrate on the form of $(h, r, ?, \mathcal{Q})$.

3.2 Qualifier Monotonicity

Let $q_1 = (h, r, ?, \mathcal{Q}_1)$ and $q_2 = (h, r, ?, \mathcal{Q}_2)$ be two queries that share the same main triple $(h, r, ?)$ and $\mathcal{Q}_1, \mathcal{Q}_2$ satisfy $\mathcal{Q}_1 \subseteq \mathcal{Q}_2$. We say that the *qualifier monotonicity property* holds over a hyper-relational knowledge graph \mathcal{G} iff $Ans(q_2, \mathcal{G}) \subseteq Ans(q_1, \mathcal{G})$, where $Ans(q_i, \mathcal{G})$ denotes the set of answers of the query q_i over \mathcal{G} . Intuitively, this property implies that adding qualifier pairs to a query does not enlarge its answer set, and conversely, removing qualifier pairs can only result in more answers. For example, consider the queries $q_1 = (James\ Harden, member_of_team, ?)$ with $\mathcal{Q}_1 = \{(start_time: 2019), (end_time: 2023)\}$ and $q_2 = (James\ Harden, member_of_team, ?)$ with $\mathcal{Q}_2 = \{(start_time: 2019), (end_time: 2023), (teammate: P.J.\ Tucker)\}$ in Figure 1. It is clear that the main triple of q_1 and q_2 are the same and $\mathcal{Q}_1 \subseteq \mathcal{Q}_2$, and the corresponding answer sets $Ans(q_1, \mathcal{G}) = \{Brooklyn\ Nets, Houston\ Rockets, Los\ Angeles\ Clippers, Philadelphia\ 76ers\}$ and $Ans(q_2, \mathcal{G}) = \{Houston\ Rockets, Los\ Angeles\ Clippers, Philadelphia\ 76ers\}$ satisfy $Ans(q_2, \mathcal{G}) \subseteq Ans(q_1, \mathcal{G})$.

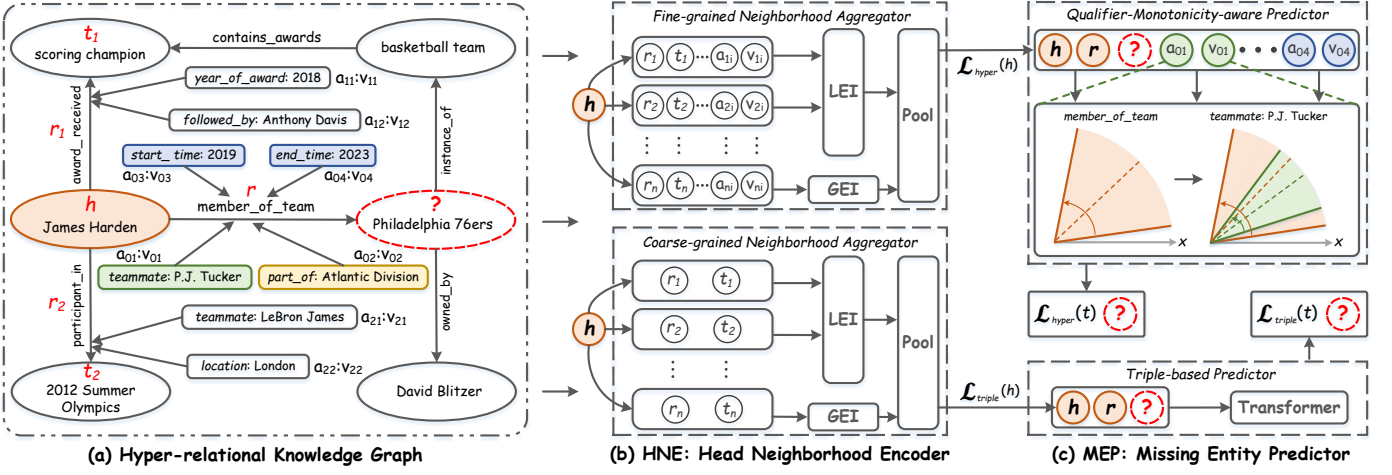


Fig. 2: HYPERMONO’s model structure, containing two modules: Head Neighborhood Encoder (HNE) and Missing Entity Predictor (MEP). HNE module contains two sub-modules: Coarse-grained Neighborhood Aggregator (CNA) and Fine-grained Neighborhood Aggregator (FNA). MEP module contains two sub-modules: Triple-based Predictor (TP) and Qualifier-Monotonicity-aware Predictor (QMP).

3.3 Cone Embedding

We present here only necessary background on cone embeddings, for a full discussion we refer the interested reader to [4], [6], [24]. A d -dimensional sector-cone can be parameterized by $\mathcal{C}^d(\alpha, \beta) = ((\alpha^1, \beta^1), \dots, (\alpha^d, \beta^d))$, where $\alpha^i \in [-\pi, \pi]$ represents the angle between the symmetry axis of the i -th-dimension sector-cone and the positive x axis, and β^i represents the aperture of the i -th-dimension sector-cone. Figure 3(a) shows a typical 1-dimensional sector-cone. We omit the superscript of \mathcal{C}^d if it is clear from context. A variety of operations on cone embeddings can be defined, here we introduce the projection \mathcal{P} and intersection \mathcal{I} operations:

- 1) *Projection Operator* \mathcal{P} . $\mathcal{C}_2 = \mathcal{P}(\mathcal{C}_1, \mathcal{C}_r)$ computes the projection from an input cone \mathcal{C}_1 as a head entity set to the set of tail entities \mathcal{C}_2 via the specific relation cone \mathcal{C}_r , see Figure 3(b). Following [4], we employ the projection operation to convert from one sector-cone to another sector-cone.
- 2) *Intersection Operator* \mathcal{I} . $\mathcal{I}(\mathcal{C}_1, \mathcal{C}_2)$ computes the intersection of the set of entities \mathcal{C}_1 and the set of entities \mathcal{C}_2 , see Figure 3(c). Considering that the intersection operation is universal in a sector-cone space (and that it is not our innovation), we directly follow the specifications defined by [4].

4 METHOD

In this section, we present the two main components of HYPERMONO’s architecture: HNE: Head Neighborhood Encoder (§ 4.1) and MEP: Missing Entity Predictor (§ 4.2). In the HNE module, we consider two types of relational contexts, and construct the sub-modules *Coarse-grained Neighbor Aggregator* and *Fine-grained Neighbor Aggregator*. In the MEP module, we introduce the *Triple-based Predictor* and *Qualifier-Monotonicity-aware Predictor* sub-modules to faithfully capture the two-stage reasoning and qualifier monotonicity properties.

4.1 HNE: Head Neighborhood Encoder

To infer the missing tail entity in the triple $(h, r, ?)$, it is important to not only consider the input embeddings of h and r , but also look at how h relates to its neighboring entities. For instance, in Figure 2(a), for the triple $(James\ Harden, member_of_team, ?)$, the relational neighbors (*award_received, scoring champion*) and (*participant_in, 2012 Summer Olympics*) of the head entity *James Harden* can help us infer that *James Harden* is an athlete and not a movie star. The same phenomenon is witnessed for hyper-relational facts $(h, r, ?, \mathcal{Q})$, i.e., we can exploit the information about how h relates to its neighbors (including or not including its qualifiers) to obtain an enhanced head entity embedding representation.

To adequately encode the content of the neighbors of a head entity, as a first step, we introduce the *Head Neighborhood Encoder (HNE)* module, cf. Figure 2(b). The HNE module considers two types of relational contexts, characterized by the use of either main triples or complete hyper-relational facts to ascertain the neighbors of a given entity: *Coarse-grained Neighbor Aggregator (CNA)*, only considering main triples in \mathcal{G}_{triple} ; *Fine-grained Neighbor Aggregator (FNA)*, considering hyper-relational facts in \mathcal{G} . The resulting neighbor-aware embeddings from the CNA and FNA modules will be used in the subsequent module (§4.2) to provide further evidence, based on the neighbors of h , for the prediction of the ? entity.

Coarse-grained Neighborhood Aggregator. For a main triple $(h, r, ?)$ from \mathcal{G}_{triple} , we use the following three steps to encode information about the neighbors of h into its representation:

- 1) *Neighbor-aware Embeddings.* Let $N_h = \{(h, r', t') \mid (h, r', t') \in \mathcal{G}_{triple}\}$ be the set of neighbors of h . For a triple $tr = (h, r', t') \in N_h$, we use the placeholder [mask] in place of h to obtain the neighbor sequence $\{[mask], r', t'\}$. Then, we apply a standard transformer encoder [39] to obtain the [mask] token embedding $N_{tr}^h \in \mathbb{R}^{1 \times d}$, d represents the embedding dimension. Clearly, if $n = |N_h|$, n different [mask] representations

will be obtained. So, we sum up and average all $[\text{mask}]$ representations to obtain an aggregated embedding N^h considering all neighbors of h : $N^h = \text{mean}(\sum_{tr \in N_h} N_{tr}^h)$.

- 2) *Local and Global Entity Inference*. Different neighbors of h might provide information about h from different perspectives. We thus propose the *Local Entity Inference (LEI)* mechanism that independently considers each neighbor to infer the entity corresponding to h . LEI focuses on a single neighbor during inference, reducing the interference from irrelevant information. In practice, for $tr \in N_h$, we perform a matrix multiplication operation on N_{tr}^h and V_{ent} to obtain the entity score vector $P_{tr}^h \in \mathbb{R}^{1 \times N} = N_{tr}^h \cdot V_{ent}^\top$, where $V_{ent} \in \mathbb{R}^{N \times d}$ denotes the embedding matrix for all entities in the dataset, V_{ent}^\top is the transpose of V_{ent} , and $N = |\mathcal{E}|$. However, in some cases, it is difficult to infer a complex entity from a single neighbor. Therefore, we additionally propose a *Global Entity Inference (GEI)* mechanism which averages the entity score vector predicted by different relational neighbors to aggregate them: $P_G^h = \text{mean}(\sum_{tr \in N_h} P_{tr}^h)$.
- 3) *Aggregating Inference Results*. The LEI and GEI mechanisms will generate multiple entity inference results, to unify them, inspired by [9], [40], we adopt an exponentially weighted pooling method to generate the final inference result:

$$P^h = \text{pool}(\{P_{tr_1}^h, P_{tr_2}^h, \dots, P_{tr_n}^h, P_G^h\}) = \sum_{i=1}^{n,G} \omega_i P_{tr_i}^h \quad (1)$$

where $\omega_i = \frac{\exp \gamma P_{tr_i}^h}{\sum_{j=1}^{n,G} \exp \gamma P_{tr_j}^h}$, γ is a hyperparameter that controls the temperature of the pooling process. We further apply a softmax function θ to P^h : $p^h = \theta(P^h)$ to map the scores between 0 and 1. Finally, we calculate the cross-entropy loss between the prediction logit p^h and the corresponding label L_1^h : $\mathcal{L}_{\text{triple}}(h) = \text{CrossEntropy}(p^h, L_1^h)$.

Fine-grained Neighborhood Aggregator. In this module, we follow similar steps as in the CNA module to obtain an aggregated representation of h , but with hyper-relational knowledge. For a hyper-relational fact $(h, r, ?, \mathcal{Q}) \in \mathcal{H}$, in the *neighbor-aware embeddings step*, after masking out h for all its neighbors, we obtain M^h defined as $= \text{mean}(\sum_{hrf \in N_{h,H}} M_{hrf}^h)$, where $N_{h,H} = \{(h, r', t', \mathcal{Q}') \mid (h, r', t', \mathcal{Q}') \in \mathcal{H}\}$. In the *local and global entity inference step*, we obtain entity inference results for all elements in $N_{h,H}$: $\{Q_{hrf_1}^h, Q_{hrf_2}^h, \dots, Q_{hrf_m}^h, Q_G^h\}$, such that $|N_{h,H}| = m$. In the *aggregating inference results step*, we also employ a pooling strategy to aggregate multiple inference results into a single prediction Q^h . Finally, we calculate the cross-entropy loss between the $q^h = \theta(Q^h)$ and the true label L_2^h as: $\mathcal{L}_{\text{hyper}}(h) = \text{CrossEntropy}(q^h, L_2^h)$.

4.2 MEP: Missing Entity Predictor

The CNA and FNA modules introduced the supervision signals $\mathcal{L}_{\text{triple}}(h)$ and $\mathcal{L}_{\text{hyper}}(h)$ for the possible values of h . However, in the hyper-relational knowledge graph completion task, the neighborhood information of the head entity h can be used as prior knowledge to infer the missing

placeholder ? results. To effectively make use of the neighborhood information, while faithfully capturing the two-stage reasoning and qualifier monotonicity properties, we introduce the *Missing Entity Predictor (MEP)* module. The *Triple-based Predictor (TF)* component of MEP accomplishes coarse-grained inferences by solely considering main triples. Based on the results from the TP sub-module, the *Qualifier-Monotonicity-aware Predictor (QMP)* subsequently obtains fine-grained inferences by considering hyper-relational facts with qualifiers, while properly representing the qualifier monotonicity property through cone embeddings. We note that the interaction between the coarse-grained and the fine-grained stages is implicitly captured through the loss function calculation. This naturally models the interaction between these stages, without having to look for ‘correct’ restrictions to explicitly capture it. We next describe the details of the TP and QMP components of MEP.

Triple-based Predictor. For an incomplete triple $(h, r, ?)$, we employ the following three steps to predict entities at the placeholder ? location: (i) We replace the placeholder ? with the $[\text{mask}]$ token to obtain input sequences $\{h, r, [\text{mask}]\}$. Further, we use the N^h embedding obtained at Step (1) of the CNA module as the input embedding of h , and randomly initialize the input embedding of r . (ii) We use a transformer encoder to obtain token embeddings $\{F^h, F^r, F^{[\text{mask}]}\}$. (iii) Finally, we use $p^t = \theta(F^{[\text{mask}]} \cdot V_{ent}^\top)$ to infer the most likely probability for entities at the mask position. Additionally, we calculate the cross-entropy loss between the prediction logit p^t and ground truth label L_1^t as $\mathcal{L}_{\text{triple}}(t) = \text{CrossEntropy}(p^t, L_1^t)$.

Qualifier-Monotonicity-aware Predictor. The previous module only considers the main triple $(h, r, ?)$ in $(h, r, ?, \mathcal{Q} = \{(a_1 : v_1), \dots, (a_s : v_s)\})$, disregarding qualifier pairs. To fully leverage the qualifier pairs information in the hyper-relational fact, building upon the qualifier monotonicity property, we propose the *Qualifier-Monotonicity-aware Predictor* module, composed of the following three sub-modules:

Token Embeddings. Like in the *triple-based predictor* module, we first replace the placeholder ? with the $[\text{mask}]$ token to obtain the input sequence $\{h, r, [\text{mask}], \{(a_1, v_1), \dots, (a_s, v_s)\}\}$. We initialize the input embedding of h using the M^h embedding obtained in the FNA module, and the remaining input embeddings of r , a_i , and v_i are randomly initialized. Then, we use a transformer encoder to obtain the output embedding representation of each token: $S = \{E^h, E^r, E^{[\text{mask}]}, \{(E^{a_1}, E^{v_1}), \dots, (E^{a_s}, E^{v_s})\}\}$.

Cone Shrinking. To faithfully capture the monotonicity property, we will resort to a geometric representation based on cone embeddings. We represent main triples as cones and each qualifier is modeled as a cone that shrinks the cone of the main triple to which the qualifier has been added. This shrinkage will be implemented through a reduction of the axis and aperture of main triples cones. Thus, our cone-based representation effectively captures that attaching qualifiers to a main triple might narrow down the answer set, but never enlarge it. Technically, our goal is to predict the most likely entity category of $E^{[\text{mask}]}$ using within the cone space the different types of token embeddings in $S = \{E^h, E^r, E^{[\text{mask}]}, \{(E^{a_1}, E^{v_1}), \dots, (E^{a_s}, E^{v_s})\}\}$. To this

aim, we introduce the *Cone Shrink Block (CSB)* module, comprising the following three steps:

- 1) We first convert the different types of token embeddings in S into the cone space. Specifically, the head entity token embedding E^h is converted to the cone $\mathcal{C}_h = \mathcal{C}(\alpha_h, \beta_h)$, and the relation to the cone $\mathcal{C}_r = \mathcal{C}(\alpha_r, \beta_r)$, with $\alpha_h, \beta_h, \alpha_r$, and β_r defined as follows:

$$\begin{cases} \alpha_h = f(\text{MLP}(E^h)), \beta_h = g(\text{MLP}(E^h)) \\ \alpha_r = f(\text{MLP}(E^r)), \beta_r = g(\text{MLP}(E^r)) \\ f(x_i) = \pi \tanh(\lambda_1 x_i), g(y_i) = \pi \tanh(\lambda_2 y_i) + \pi \end{cases} \quad (2)$$

where $\text{MLP}: \mathbb{R}^d \rightarrow \mathbb{R}^d$ is a multi-layer perceptron network, the functions f and g are used to scale the semantic center axis and aperture into their normal ranges: $\alpha_h = f(\mathbf{x}) = [\alpha_h^1, \dots, \alpha_h^d; \alpha_h^i = f(x_i)]$, α_h^i and $f(x_i)$ denote the i -th element of α_h and $f(\mathbf{x})$; $\beta_h = g(\mathbf{y}) = [\beta_h^1, \dots, \beta_h^d; \beta_h^i = g(y_i)]$, β_h^i and $g(y_i)$ denote the i -th element of β_h and $g(\mathbf{y})$, λ_1 and λ_2 are two scaling hyper-parameters. α_r and β_r are defined similarly.

We then map the embedding region of the head entity set \mathcal{C}_h to the entity set $\mathcal{C}_{h,r}$ through a relation-dependent projection operation $\mathcal{P}: \mathcal{C}_{h,r} = \mathcal{C}(\alpha_{h,r}, \beta_{h,r}) = \mathcal{P}(\mathcal{C}_h, \mathcal{C}_r)$.

- 2) As discussed, the monotonicity property can be intuitively captured by reducing the axis and aperture of main triple cones to which qualifiers are added. More precisely, to geometrically represent this property in the cone embedding space, we model each qualifier ($a_i : v_i$) as a shrinking of a cone. The spatial representation is such that the cone obtained after shrinking is a sub-cone of the original one. For example, in Figure 3(d), the shrink cone \mathcal{C}_2 is a subset of the original cone \mathcal{C}_1 . Given a cone $\mathcal{C}(\alpha_{h,r}, \beta_{h,r})$ obtained in the previous step and the token embedding (E^{a_i}, E^{v_i}) of the i -th qualifier pair, we formally define a cone-to-cone shrink transformation from $\mathcal{C}(\alpha_{h,r}, \beta_{h,r})$ to $\mathcal{C}(\alpha_{\mathcal{S}_i}, \beta_{\mathcal{S}_i})$ using Equation (3) below. Intuitively, Equation (3) adjusts the source angle of axis $\alpha_{h,r}$ and the aperture $\beta_{h,r}$ to shrink them to $\alpha_{\mathcal{S}_i}$ and $\beta_{\mathcal{S}_i}$, respectively, ensuring that the resulting cone is contained in the original cone.

$$\begin{cases} \alpha_{r,a_i,v_i} = f(\text{MLP}_1(\Theta_{r,a_i,v_i})) \\ \beta_{r,a_i,v_i} = g(\text{MLP}_1(\Theta_{r,a_i,v_i})) \\ \text{offset} = (\beta_{h,r} - \beta_{\mathcal{S}_i}) \odot \sigma(\alpha_{r,a_i,v_i}), \beta_{\mathcal{S}_i} = \sigma(\beta_{r,a_i,v_i}) \\ \alpha_{\mathcal{S}_i} = \alpha_{h,r} - 0.5 \odot \beta_{h,r} + 0.5 \odot \beta_{\mathcal{S}_i} + 0.5 \odot \text{offset} \end{cases} \quad (3)$$

where $\Theta_{r,a_i,v_i} = \text{MLP}_2(\text{Concat}(E^r, E^{a_i}, E^{v_i}))$, which leverages an MLP layer which takes the primary relation and attribute-value qualifier as input, and outputs the combined representation of relational and hyper-relational knowledge. $\text{MLP}_1: \mathbb{R}^d \rightarrow \mathbb{R}^d$ and $\text{MLP}_2: \mathbb{R}^{3d} \rightarrow \mathbb{R}^d$ are multi-layer perceptron networks, σ is a sigmoid function and \odot is the element-wise vector multiplication.

From Equation (3), we obtain a sector-cone $\mathcal{C}_{\mathcal{S}_i} = \mathcal{C}(\alpha_{\mathcal{S}_i}, \beta_{\mathcal{S}_i})$ that has been shrunk by the qualifier ($a_i : v_i$).

- 3) After obtaining a scaled down sector-cone $\mathcal{C}_{\mathcal{S}_i}$, for each i -th qualifier, we obtain s independent cones:

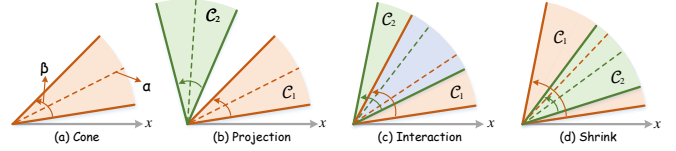


Fig. 3: An overview of cone embedding with projection \mathcal{P} , intersection \mathcal{I} and shrink \mathcal{S} , the embedding dimension $d=1$.

$\{\mathcal{C}_{\mathcal{S}_1}, \dots, \mathcal{C}_{\mathcal{S}_s}\}$. Finally, when considering multiple qualifier pairs at the same time, the answer set can be computed by the cone intersection operation $\mathcal{I}: \mathcal{C}_{\mathcal{S}} = (\alpha_{\mathcal{S}}, \beta_{\mathcal{S}}) = \mathcal{I}(\mathcal{C}_{\mathcal{S}_1}, \dots, \mathcal{C}_{\mathcal{S}_s})$.

Inference Results. We apply $\mathbf{q}^t = \theta(\text{MLP}(\text{Concat}(\alpha_{\mathcal{S}}, \beta_{\mathcal{S}})) \cdot \mathbf{V}_{ent}^T)$ to change the answer cone $\mathcal{C}_{\mathcal{S}}$ to the entity probability at the ? position. Additionally, we calculate the cross-entropy loss between the prediction score \mathbf{q}^t and the label L_2^t as $\mathcal{L}_{hyper}(t) = \text{CrossEntropy}(\mathbf{q}^t, L_2^t)$.

4.3 Joint Training

We combine the loss functions obtained above into a joint loss function:

$$\mathcal{L}_{joint} = \mathcal{L}_{triple}(h) + \mathcal{L}_{hyper}(h) + \mathcal{L}_{triple}(t) + \mathcal{L}_{hyper}(t) \quad (4)$$

5 EXPERIMENTS

To evaluate the effectiveness of our model, we aim to explore the following five research questions:

- **RQ1 (Effectiveness):** How our model performs compared to the state-of-the-art under different conditions?
- **RQ2 (Ablation studies):** How different components contribute to its performance?
- **RQ3 (Model transferability):** Can HYPERMONO be used to complete hypergraphs?
- **RQ4 (Parameter sensitivity):** How hyper-parameters influence its performance?
- **RQ5 (Complexity analysis):** What is the amount of computation and parameters used by HYPERMONO?

5.1 Experiment Setup

5.1.1 Datasets

We conduct experiments on three hyper-relational KGs: WD50K [17], WikiPeople [41], and JF17K [13], with WD50K and WikiPeople being extracted from Wikidata [42] and JF17K from Freebase [43]. These datasets have the following two characteristics. On the one hand, *not* all main triples contain hyper-relational knowledge: only 13.6% in WD50K, 2.6% in WikiPeople and 45.9% in JF17K. On the other hand, each main triple has a different number of qualifier pairs: ranging from 0 to 20 in WD50K, 0 to 7 in WikiPeople and 0 to 4 in JF17K. To validate the models' robustness across multiple scenarios, these datasets have been refined taking into account the two described characteristics [23], i.e., the percentage of triples containing hyper-relational knowledge (mixed-percentage or fixed-percentage) and the number of qualifiers associated to main triples (mixed-qualifier or fixed-qualifier). We can thus construct three different sub-datasets, namely: *Mixed-percentage Mixed-qualifier*,

Fixed-percentage Mixed-qualifier, and *Fixed-percentage Fixed-qualifier*. Note that the by definition *Mixed-percentage Fixed-qualifier scenario does not exist*. The statistics of the considered datasets are as shown in the Table 1.

- 1) *Mixed-percentage Mixed-qualifier*. This is the original setting introduced in [17], used to test the performance under variable number of main triples with qualifiers and with different number of qualifiers associated to those triples.
- 2) *Fixed-percentage Mixed-qualifier*. Following [17], [23], we construct subsets where the number of qualifiers for each triple varies, but the proportion of triples with hyper-relational knowledge is fixed. For example, in the subsets WD50K (33), WD50K (66), and WD50K (100), the number in parentheses indicates the corresponding proportion of main triples with hyper-relational knowledge. We consider similar subsets for the WikiPeople and JF17K datasets.
- 3) *Fixed-percentage Fixed-qualifier*. Considering the monotonicity of this representational regime, we filter out the triples with 3 and 4 associated qualifiers to obtain WikiPeople-3, WikiPeople-4, JF17K-3, and JF17K-4.

TABLE 1: Statistics of datasets under three different scenarios. The values in parentheses indicate the percentage of triples in the corresponding dataset with hyper-relational facts. The hyphen $-n$ indicates that each main triple in the corresponding dataset contains n qualifier pairs.

Datasets	Train	Valid	Test	Entity	Relation
WD50K	166435	23913	46159	47155	531
WikiPeople	294439	37715	37712	34825	178
JF17K	76379	-	24568	28645	501
WD50K (33)	73406	10568	18133	38123	474
WD50K (66)	35968	5154	8045	27346	403
WD50K (100)	22738	3279	5297	18791	278
WikiPeople (33)	28280	3550	3542	20921	145
WikiPeople (66)	14130	1782	1774	13651	133
WikiPeople (100)	9319	1181	1173	8068	105
JF17K (33)	56959	8122	9112	24081	490
JF17K (66)	27280	4413	5403	19288	469
JF17K (100)	17190	3152	4142	12656	307
WikiPeople-3	20656	2582	2582	12270	66
WikiPeople-4	12150	1519	1519	9528	50
JF17K-3	27635	3454	3455	11541	104
JF17K-4	7607	951	951	6536	23

5.1.2 Baselines, Evaluation Protocol and Implementation Details

Baselines. We compare HYPERMONO with twelve state-of-the-art baselines for HKGC, including **Embedding-based Methods**, **Transformer-based with GNNs Methods**, and **Transformer-based without GNNs Methods**:

The **Embedding-based Methods** include:

- *m-TransH* [13] builds on TransH by transforming each hyper-relational fact using a star-to-clique conversion.
- *RAE* [14] integrates m-TransH with a multi-layer perceptron by considering the relatedness of entities. However,

since the distance-based scoring function of TransH enforces constraints on relations, it fails to represent some binary relations in KGs.

- *NaLP-Fix* [15] uses a convolutional-based framework to compute a relatedness vector for a triple. However, the model does not distinguish between the main triple and relation-specific qualifiers.
- *HINGE* [15] adopts a convolutional framework for modeling hyper-relational facts. However, it only operates on a triple-quintuple level that lacks the necessary granularity for representing a relation instance with its qualifiers.
- *ShrinkE* [16] models the primary triplets as a spatial-functional transformation from the head into a relation-specific box.

The **Transformer-based with GNNs Methods** include:

- *StarE* [17] employs a message passing based graph encoder to obtain entity/relation embeddings, and feeds these embeddings to a transformer decoder to score hyper-relational facts.
- *QUAD* [18] introduces a graph encoder that aggregates information from the perspective of the qualifier entities. There are two variants of QUAD: QUAD and QUAD (Parallel). If there is no special suffix, QUAD denotes QUAD (Parallel).

The **Transformer-based without GNNs Methods** include:

- *HyTrans* [19] replaces the graph encoder with light-weight embedding modules, achieving higher efficiency without sacrificing effectiveness.
- *GRAN* [20] represents a fact as a heterogeneous graph, and employs edge-specific attentive bias to capture both local and global dependencies within the given fact. Note that GRAN contains three variants, i.e., GRAN-hete is the full model, GRAN-homo retains the graph structure but ignores heterogeneity and GRAN-complete considers neither the graph structure nor heterogeneity. If there is no special suffix, GRAN denotes GRAN-hete.
- *HyNT* [21] proposes a unified framework that learns representations of a hyper-relational knowledge graph containing numeric literals in either triples or qualifiers.
- *HAHE* [22] presents a model with hierarchical attention in global and local level to encode the graphical structure and sequential structure via self-attention layers.
- *HyperFormer* [23] considers local-level sequential information to encode the content of entities, relations and qualifiers. It includes an entity neighbor aggregator, relation qualifier aggregator and convolution-based bidirectional interaction modules.

Evaluation Protocol. Following existing work [16], [21], [22], [23], we rank all entities to predict the head entity in query $(?, r, t, \mathcal{Q})$ or the tail entity in query $(h, r, ?, \mathcal{Q})$. Specifically, we employ MRR and Hits@ k (abbreviated sometimes as $H@k$, $k \in \{1, 3, 10\}$) as evaluation metrics. MRR defines the inverse of the rank for the first correct answer, while Hits@ k calculates the percentage of correct types ranked among the top- k answers. For all metrics, the larger the value, the better. Following the standard evaluation protocol in the filtered setting [1], all true triples in the HKGs are filtered out during evaluation, since predicting

TABLE 2: Evaluation of different models under the mixed-percentage mixed-qualifier scenario on the WD50K, WikiPeople and JF17K datasets. All baseline results are collected from the original papers. Best scores are highlighted in **bold**, the second best scores are underlined, and ‘-’ indicates the results are not reported in previous work. The number in parentheses represents the proportion of triples with hyper-relational knowledge.

Methods	WD50K (13.6)			WikiPeople (2.6)			JF17K (45.9)		
	MRR	Hits@1	Hits@10	MRR	Hits@1	Hits@10	MRR	Hits@1	Hits@10
<i>Embedding-based Methods</i>									
m-TransH [13]	-	-	-	0.063	0.063	0.300	0.206	0.206	0.463
RAE [14]	-	-	-	0.059	0.059	0.306	0.215	0.215	0.469
NaLP-Fix [15]	0.177	0.131	0.264	0.420	0.343	0.556	0.245	0.185	0.358
HINGE [15]	0.243	0.176	0.377	0.476	0.415	0.585	0.449	0.361	0.624
ShrinkE [16]	0.345	0.275	0.482	0.485	0.431	0.601	0.589	0.506	0.749
<i>Transformer-based with GNNs Methods</i>									
StarE [17]	0.349	0.271	0.496	0.491	0.398	0.648	0.574	0.496	0.725
QUAD [18]	0.348	0.270	0.497	0.466	0.365	0.624	0.582	0.502	0.740
QUAD (Parallel) [18]	0.349	0.275	0.489	0.497	0.431	0.617	0.596	0.519	0.751
<i>Transformer-based without GNNs Methods</i>									
HyTrans [19]	0.356	0.281	0.498	0.501	0.426	0.634	0.582	0.501	0.742
GRAN-hete [20]	-	-	-	<u>0.503</u>	<u>0.438</u>	0.620	0.617	0.539	0.770
GRAN-homo [20]	-	-	-	0.487	0.410	0.618	0.611	0.533	0.767
GRAN-complete [20]	-	-	-	0.489	0.413	0.617	0.591	0.510	0.753
HyNT [21]	0.314	0.241	0.454	0.464	0.380	0.601	0.554	0.475	0.711
HAHE [22]	<u>0.368</u>	<u>0.291</u>	<u>0.516</u>	0.509	0.447	0.639	0.623	0.554	0.806
HyperFormer [23]	0.366	0.288	0.514	0.491	0.386	<u>0.654</u>	<u>0.664</u>	<u>0.601</u>	0.787
HYPERMONO	0.375	0.298	0.522	0.494	0.390	0.657	0.685	0.630	<u>0.796</u>

a low rank for these triples should not be penalized. All metrics are computed by averaging over two directions: head entity prediction and tail entity prediction.

Implementation Details. We conduct all experiments on six 32G Tesla V100 GPUs, and employ the AdamW [44] optimizer and a cosine decay scheduler with a linear warm-up for optimization. The hyperparameters are tuned according to the MRR on the validation set. We use grid search to select the optimal hyperparameters, mainly including: the learning rate $lr \in \{3e-4, 4e-4, 5e-4, \mathbf{6e-4}, 7e-4\}$, the label smooth values $ls \in \{0.3, 0.4, 0.5, 0.6, 0.7, \mathbf{0.8}, 0.9\}$, the embedding dimension $d \in \{50, 100, 150, \mathbf{200}, 400, 600\}$, the temperature of Equation (1) $\gamma \in \{1, 2, 3, \mathbf{4}, 5, 6\}$, the initialization range of embeddings $ir \in \{0.01, \mathbf{0.02}, 0.05, 0.1, 0.2, 0.35, 0.5\}$, the neighbors of the head entity $\{2, 3, 4\}$, the number of qualifiers for a relation $\{5, 6, 7\}$, the number of layers in the transformer $\{2, 4, \mathbf{8}\}$, the number of heads in transformer $\{1, 2, 4, \mathbf{8}\}$, the input dropout rate in the transformer $\{0.6, \mathbf{0.7}, 0.8\}$.

5.2 Main Results

To address **RQ1**, we conduct experiments on the three types of datasets described above. The corresponding results are shown in Tables 2, 3, and 4.

Mixed-percentage Mixed-qualifier. Table 2 summarizes the results on WD50K, WikiPeople, and JF17K under the mixed-percentage mixed-qualifier condition. We can observe that HYPERMONO outperforms existing SoTA baselines by a large margin across most metrics on WD50K and JF17K. In

particular, when compared with HyperFormer (the best performing baseline), HYPERMONO respectively achieves 2.1% and 2.9% improvements in MRR and Hits@1 on the JF17K dataset. A similar phenomenon occurred on the WD50K dataset. However, for the WikiPeople dataset, even though we can achieve optimal performance on the Hits@10 metric, we cannot surpass the best performing baseline on MRR and Hits@1. The intuitive reason for this is that, in comparison to the WD50K and JF17K datasets where 13.6% and 45.9% of main triple respectively contain hyper-relational knowledge, only 2.6% of triples in WikiPeople have qualifier pairs. This hinders HYPERMONO’s ability to exploit stage reasoning and qualifier monotonicity. Specifically, we employ a scaling transformation in the cone space to capture qualifier monotonicity, but the lack of qualifier pairs constrains this functionality.

Fixed-percentage Mixed-qualifier. Table 3 presents the results on WD50K, WikiPeople, and JF17K under different fixed ratios of relational facts with qualifiers. For each dataset, we construct three subsets (as describe in § 5.1.1, Point 2) containing approximately 33%, 66%, and 100% of facts with qualifiers. We observe that under different proportions of hyper-relational knowledge HYPERMONO also achieves optimal performance. Particularly, for the WikiPeople dataset, in which HYPERMONO performs poorly in the mixed-percentage mixed-qualifier scenario, adding a certain percentage of qualifiers information to triples results in HYPERMONO outperforming all baselines. For example, for the Hits@1 metric, HYPERMONO respectively achieves improvements over the best performing base-

TABLE 3: Evaluation of different models under the fixed-percentage mixed-qualifier scenario on the WD50K, WikiPeople and JF17K datasets. Best scores are highlighted in **bold**, the second best scores are underlined. QUAD denotes the QUAD (Parallel) model in Table 2, and GRAN denotes the GRAN-hete model in Table 2.

Methods	WD50K						WikiPeople						JF17K					
	33%		66%		100%		33%		66%		100%		33%		66%		100%	
	MRR	H@1	MRR	H@1	MRR	H@1	MRR	H@1	MRR	H@1	MRR	H@1	MRR	H@1	MRR	H@1	MRR	H@1
<i>Embedding-based Methods</i>																		
ShrinkE	0.246	0.190	0.356	0.294	0.470	0.404	0.176	0.129	0.244	0.198	0.332	0.276	0.259	0.176	0.263	0.185	0.299	0.220
<i>Transformer-based with GNNs Methods</i>																		
StarE	0.308	0.247	0.449	0.388	0.610	0.543	0.192	0.143	0.259	0.205	0.343	0.279	0.290	0.197	0.302	0.214	0.321	0.223
QUAD	0.329	0.266	0.479	0.416	0.646	0.572	0.204	0.155	0.282	0.228	0.385	0.318	0.307	0.210	0.334	0.241	0.379	0.277
<i>Transformer-based without GNNs Methods</i>																		
HyTrans	0.313	0.255	0.458	0.397	0.621	0.557	0.192	0.140	0.268	0.215	0.372	0.316	0.298	0.204	0.325	0.234	0.361	0.266
GRAN	0.322	<u>0.269</u>	0.472	0.419	0.647	0.593	0.201	0.156	0.287	0.244	0.403	0.349	0.307	0.212	0.326	0.237	0.382	0.290
HyNT	0.295	0.238	0.438	0.377	0.595	0.525	0.175	0.130	0.243	0.192	0.329	0.269	0.285	0.195	0.298	0.216	0.352	0.261
HAHE	0.301	0.239	0.432	0.368	0.607	0.537	0.188	0.142	0.263	0.213	0.367	0.304	0.311	0.221	0.330	0.248	0.387	0.293
HyperFormer	<u>0.338</u>	0.280	0.492	0.434	<u>0.666</u>	<u>0.611</u>	<u>0.213</u>	<u>0.161</u>	<u>0.298</u>	<u>0.255</u>	<u>0.426</u>	<u>0.373</u>	<u>0.352</u>	<u>0.254</u>	<u>0.411</u>	<u>0.325</u>	<u>0.478</u>	<u>0.396</u>
HYPERMONO	0.341	0.280	<u>0.490</u>	<u>0.433</u>	0.667	0.612	0.221	0.173	0.309	0.264	0.427	0.379	0.357	0.267	0.423	0.340	0.493	0.408

TABLE 4: Evaluation of different models under the fixed-percentage fixed-qualifier scenario on the WikiPeople and JF17K datasets. Best scores are highlighted in **bold**, the second best scores are underlined. QUAD denotes the QUAD (Parallel) model in Table 2, and GRAN denotes the GRAN-hete model in Table 2.

Methods	WikiPeople-3				WikiPeople-4				JF17K-3				JF17K-4			
	MRR	H@1	H@3	H@10	MRR	H@1	H@3	H@10	MRR	H@1	H@3	H@10	MRR	H@1	H@3	H@10
<i>Embedding-based Methods</i>																
ShrinkE	0.366	0.291	0.397	0.515	0.222	0.155	0.252	0.353	0.712	0.648	0.745	0.837	0.779	0.726	0.809	0.886
<i>Transformer-based with GNNs Methods</i>																
StarE	0.401	0.310	0.434	0.592	0.243	0.156	0.269	0.430	0.707	0.635	0.744	0.847	0.723	0.669	0.753	0.839
QUAD	0.403	0.321	0.438	0.563	0.251	0.167	0.280	0.425	0.730	0.660	0.767	0.870	0.787	0.730	0.823	0.895
<i>Transformer-based without GNNs Methods</i>																
HyTrans	0.403	0.323	0.436	0.569	0.248	0.165	0.275	0.422	0.690	0.617	0.725	0.837	0.773	0.717	0.806	0.875
GRAN	0.397	0.328	0.429	0.533	0.239	0.178	0.261	0.364	0.779	0.724	0.811	0.893	0.798	0.744	0.830	0.904
HyNT	0.383	0.306	0.415	0.533	0.233	0.166	0.257	0.369	0.733	0.664	0.771	0.873	0.779	0.725	0.809	0.881
HAHE	0.397	0.323	0.432	0.537	0.251	0.179	0.286	0.392	0.762	0.701	0.791	0.892	0.736	0.666	0.773	0.869
HyperFormer	0.573	<u>0.511</u>	<u>0.603</u>	0.693	<u>0.393</u>	<u>0.336</u>	0.415	0.496	0.832	0.790	<u>0.855</u>	<u>0.914</u>	<u>0.857</u>	<u>0.811</u>	<u>0.884</u>	<u>0.937</u>
HYPERMONO	0.586	0.531	0.611	<u>0.690</u>	0.398	0.359	<u>0.408</u>	<u>0.474</u>	0.867	0.839	0.880	0.927	0.881	0.847	0.901	0.945

line, HyperFormer, of 1.2% / 0.9% / 0.6% in the 33% / 66% / 100% variants. This confirms that the proportion of hyper-relational knowledge is a major factor influencing the performance over WikiPeople under the mixed-percentage mixed-qualifier condition. In contrast, on the WD50K dataset, no significant additional improvement was obtained. The most likely reason is the insufficient richness of hyper-relational knowledge in WD50K. For example, in WD50k_100 65.23% of the triples only contain *one* hyper-relation pair, which limits the functionality of qualifier monotonicity module.

Fixed-percentage Fixed-qualifier. To better understand the impact of hyper-knowledge on the performance, we consider the WikiPeople and JF17K datasets with a fixed number of qualifiers, cf. Table 4. We can observe that HYPERMONO consistently achieves optimal performance on almost all datasets. Specifically, in terms of the MRR metric, HYPERMONO respectively shows improvements of

3.5% and 2.4% on the JF17K-3 and JF17K-4 subsets when compared with HyperFormer. Furthermore, we find that for all models, their performance in the fixed-percentage fixed-qualifier setting is generally higher than in the fixed-percentage mixed-qualifier one. The main reason is that in the fixed-percentage fixed-qualifier scenario, the number of qualifier pairs for each triple is fixed, and there is no imbalance in the distribution of hyper-relational knowledge, which further makes the model training process more stable. Therefore, we can conclude that, in general, ensuring a relative stability of hyper-relational knowledge for each triple positively impacts the performance.

5.3 Ablation Studies

To address **RQ2**, we conduct ablation experiments on WikiPeople-3, WikiPeople-4, JF17K-3, and JF17K-4 subsets to verify the contribution of each component of HYPERMONO. These include the following three aspects: a)

TABLE 5: Ablation studies about different components. Best scores are highlighted in **bold**.

Methods	WikiPeople-3				WikiPeople-4				JF17K-3				JF17K-4			
	MRR	H@1	H@3	H@10	MRR	H@1	H@3	H@10	MRR	H@1	H@3	H@10	MRR	H@1	H@3	H@10
w/o CNA+TP	0.559	0.493	0.591	0.686	0.367	0.305	0.387	0.484	0.832	0.792	0.855	0.912	0.860	0.820	0.885	0.940
w/o FNA+QMP	0.560	0.510	0.578	0.663	0.377	0.340	0.383	0.445	0.839	0.811	0.848	0.900	0.842	0.809	0.859	0.909
w/o LEI	0.576	0.523	0.599	0.678	0.394	0.359	0.400	0.465	0.860	0.834	0.871	0.918	0.878	0.843	0.898	0.946
w/o GEI	0.584	0.532	0.608	0.690	0.396	0.355	0.404	0.471	0.866	0.838	0.878	0.926	0.883	0.852	0.900	0.949
w/o CSB	0.565	0.502	0.595	0.687	0.355	0.296	0.380	0.464	0.831	0.789	0.853	0.915	0.854	0.815	0.881	0.933
HYPERMONO	0.586	0.531	0.611	0.690	0.398	0.359	0.408	0.474	0.867	0.839	0.880	0.927	0.881	0.847	0.901	0.945

TABLE 6: Evaluation of the *knowledge hypergraph completion task* in the mixed arity setting on the N-WikiPeople, N-JF17K and N-FB-AUTO datasets. Best scores are highlighted in **bold**, the second best scores are underlined.

Methods	N-WikiPeople				N-JF17K				N-FB-AUTO			
	MRR	H@1	H@3	H@10	MRR	H@1	H@3	H@10	MRR	H@1	H@3	H@10
RAE [14]	0.253	0.118	0.343	0.463	0.396	0.312	0.433	0.561	0.703	0.614	0.764	0.854
NaLP [41]	0.338	0.272	0.364	0.466	0.310	0.239	0.334	0.450	0.672	0.611	0.712	0.774
HINGE [15]	0.333	0.259	0.361	0.477	0.473	0.397	0.490	0.618	0.678	0.630	0.706	0.765
NeuInfer [31]	0.350	0.282	0.381	0.467	0.451	0.373	0.484	0.604	0.737	0.700	0.755	0.805
HypE [26]	0.263	0.127	0.355	0.486	0.494	0.399	0.532	0.650	0.804	0.774	0.824	0.856
RAM [30]	0.380	0.279	0.455	0.539	0.539	0.463	0.573	0.690	0.830	0.803	0.851	0.876
HyperMLN [45]	0.351	0.270	0.394	0.497	0.556	0.482	0.597	0.717	0.831	0.803	0.851	0.877
tNaLP+ [46]	0.339	0.269	0.369	0.473	0.449	0.370	0.484	0.598	0.729	0.645	0.748	0.826
S2S [47]	0.372	0.277	0.439	0.533	0.528	0.457	0.570	0.690	-	-	-	-
HyConvE [48]	0.362	0.275	0.388	0.501	<u>0.590</u>	0.478	0.610	0.729	0.847	0.820	0.872	0.901
MSeaKG [32]	0.392	0.290	0.468	0.553	0.561	0.475	0.591	0.705	-	-	-	-
HJE [49]	<u>0.450</u>	<u>0.375</u>	<u>0.487</u>	<u>0.582</u>	<u>0.590</u>	<u>0.507</u>	0.613	0.729	<u>0.872</u>	0.848	0.886	0.903
PolygonE [50]	0.431	0.334	0.454	0.568	0.565	0.485	0.602	0.708	0.858	0.826	0.871	<u>0.921</u>
HyCubE [51]	0.438	0.358	0.482	0.575	0.581	<u>0.507</u>	<u>0.615</u>	<u>0.731</u>	0.884	0.863	<u>0.897</u>	0.920
HYPERMONO	0.481	0.381	0.545	0.637	0.676	0.612	0.708	0.801	0.884	<u>0.855</u>	0.907	0.937

whether the knowledge of qualifiers is considered to infer missing entities, see rows “w/o CNA+TP” and “w/o FNA+QMP” in Table 5; b) different neighbor aggregation strategies, see rows “w/o LEI” and “w/o GEI” in Table 5; c) without the cone shrink operation in QMP, see row “w/o CSB” in Table 5.

Different Variants of HYPERMONO. In Table 5, we observe that under most metrics removing any functional module will bring some performance degradation, which justifies the necessity of each component. Specifically:

- 1) removing either CNA+TP, which are related to coarse-grained answer prediction, or FNA+QMP, which are related to with fine-grained answer prediction, will result in a significant loss of accuracy. The intuitive reason is that the coarse-grained answer set can be used to constrain the decision space of fine-grained answers, preventing the occurrence of answer drift. Meanwhile, the fine-grained answer set allows to refine the answer set, ensuring the reliability of the predicted results.
- 2) The neighborhood information of known entities has a positive effect on predicting missing entities, and the use of LEI for integrating the neighbors of known entities has a greater impact on inference than GEI.
- 3) Removing the CSB module will bring a significant decrease in performance. The main reason is that the CSB

module captures the qualifier monotonicity of hyper-relational KGs. The main characteristic of the HKGC task is the application of qualifier knowledge in triples to infer answer sets. Through the natural scaling transformation of the cone space, it can be captured that attaching qualifiers to a triple can only narrow down the answer set, but never enlarge it.

5.4 Knowledge Hypergraph Completion

To address RQ3, we further validate the transfer ability of HYPERMONO. To this aim, we also conduct experiments on the Knowledge Hypergraph Completion (KHC) task. We start by introducing the task definition, dataset descriptions, and baselines. We only introduce necessary background, for a detailed discussion, interested readers are directed to the relevant literatures [32], [47], [48], [49], [50], [51].

Task Definition. A *knowledge hypergraph graph* \mathcal{G} is defined as $\{\mathcal{E}, \mathcal{R}, \mathcal{T}\}$, where \mathcal{E} is a set of entities, \mathcal{R} is a set of relation types and \mathcal{T} is a set of facts of the form $r(e_1, e_2, \dots, e_n)$ with $r \in \mathcal{R}$, $e_i \in \mathcal{E}$, for all $i \in [1, n]$ and n is the non-negative arity of r , representing the number of entities involved within each relation. The *Knowledge Hypergraph Completion (KHC)* task looks at predicting a missing entity in the i -th position of the tuple $r(e_1, e_2, \dots, ?, \dots, e_{n-1}, e_n)$. Note that the KHC generalizes the HKGC task in the sense that we

TABLE 7: Evaluation of the *knowledge hypergraph completion task* in the fixed arity setting on the N-WikiPeople-3, N-WikiPeople-4, N-JF17K-3 and N-JF17K-4 datasets. Best scores are highlighted in **bold**, the second best scores are underlined.

Methods	N-WikiPeople-3				N-WikiPeople-4				N-JF17K-3				N-JF17K-4			
	MRR	H@1	H@3	H@10	MRR	H@1	H@3	H@10	MRR	H@1	H@3	H@10	MRR	H@1	H@3	H@10
RAE [14]	0.239	0.168	0.252	0.379	0.150	0.080	0.149	0.273	0.505	0.430	0.532	0.644	0.707	0.636	0.751	0.835
NaLP [41]	0.301	0.226	0.327	0.445	0.342	0.237	0.400	0.540	0.515	0.431	0.552	0.679	0.719	0.673	0.742	0.805
HINGE [15]	0.338	0.255	0.360	0.508	0.352	0.241	0.419	0.557	0.587	0.509	0.621	0.738	0.745	0.700	0.775	0.842
NeuInfer [31]	0.355	0.262	0.388	0.521	0.361	0.255	0.424	0.566	0.622	0.533	0.658	0.770	0.765	0.722	0.808	0.871
HypE [26]	0.266	0.183	-	0.443	0.304	0.191	-	0.527	0.364	0.255	-	0.573	0.408	0.300	-	0.627
RAM [30]	0.254	0.190	-	0.383	0.226	0.161	-	0.367	0.578	0.505	-	0.722	0.743	0.701	-	0.845
HyperMLN [45]	0.252	0.193	-	0.385	0.224	0.167	-	0.370	0.574	0.501	-	0.711	0.734	0.687	-	0.831
tNaLP+ [46]	0.270	0.185	-	0.444	0.344	0.223	-	0.578	0.411	0.325	-	0.617	0.630	0.531	-	0.722
S2S [47]	0.386	0.299	<u>0.421</u>	0.559	0.391	0.270	<u>0.470</u>	0.600	0.740	<u>0.676</u>	<u>0.770</u>	0.860	0.822	0.761	<u>0.853</u>	0.924
HyConvE [48]	0.318	0.240	-	0.482	0.386	0.271	-	0.607	0.729	<u>0.670</u>	-	0.861	0.827	0.770	-	0.931
MSeaKG [32]	<u>0.403</u>	-	-	0.579	<u>0.409</u>	-	-	<u>0.624</u>	<u>0.754</u>	-	-	<u>0.889</u>	<u>0.833</u>	-	-	<u>0.938</u>
HJE [49]	0.381	<u>0.303</u>	-	<u>0.596</u>	0.388	<u>0.276</u>	-	0.607	0.707	0.637	-	0.851	0.827	<u>0.775</u>	-	0.928
HyCubE [51]	0.322	0.247	-	0.469	0.370	0.252	-	0.583	0.615	0.544	-	0.752	0.792	0.744	-	0.879
HYPERMONO	0.454	0.375	0.486	0.611	0.486	0.395	0.545	0.650	0.793	0.739	0.824	0.901	0.888	0.855	0.910	0.951

predict entities in any position, not only in the head or tail ones.

Datasets. We test the performance of HYPERMONO on the KHC task. We conduct experiments on hypergraphs with *mixed arity*: N-WikiPeople, N-JF17K, and N-FB-AUTO and with *fixed arity*: N-WikiPeople-3, N-WikiPeople-4, N-JF17K-3, and N-JF17K-4. The statistics of the corresponding datasets are consistent with existing literatures [32], [47], [48], [49], [50], [51].

Baselines. For knowledge hypergraph completion task, we select 14 state-of-the-art baselines, including RAE [14], NaLP [41], HINGE [15], NeuInfer [31], HypE [26], RAM [30], HyperMLN [45], tNaLP+ [46], S2S [47], HyConvE [48], MSeaKG [32], HJE [49], PolygonE [50], and HyCubE [51].

Performance Analysis. The results of the knowledge hypergraph completion experiments in the mixed arity and fixed arity settings are respectively shown in Table 6 and Table 7. We observe that our HYPERMONO consistently achieves state-of-the-art performance on all benchmark datasets. For the mixed arity scenario, compared with the best-performing baseline HyCubE, HYPERMONO obtains improvements of 4.3% on N-WikiPeople and 9.5% on N-JF17K in the MRR metric. On the N-FB-AUTO dataset, HYPERMONO virtually matches the results of the best performing baseline. These results demonstrate the capability and effectiveness of HYPERMONO for capturing and extracting various types of information and knowledge. The same phenomenon occurs in the fixed arity scenario, HYPERMONO respectively obtains performance improvements of 13.2%, 11.6%, 17.8%, and 9.6% in the MRR metric on the N-WikiPeople-3, N-WikiPeople-4, N-JF17K-3, and N-JF17K-4 datasets, when compared with the best baseline HyCubE. Such a notable performance improvement is mainly due to our explicit treatment of qualifier monotonicity during the encoding process. This feature is more suitable for scenarios where arity is fixed, because introducing qualifier monotonicity can greatly reduce the scope of the optional answer space to obtain the final answer.

5.5 Parameter Sensitivity

To address RQ4, we carry out parameter sensitivity experiments on the WikiPeople-4 and JF17K-3 datasets, including: a) effect of label smoothing; b) effect of embedding dimension d ; c) effect of temperature γ , and d) effect of initialization range. The corresponding results are shown in Figure 4.

Effect of Label Smoothing. Label smoothing is widely used in tasks related to knowledge graphs [52], [53], [54]. It introduces a degree of uncertainty, making the model more adaptable to different data distributions during the training process and further suppresses model overconfidence and improves its generalization ability and robustness. From Figure 4(a), we observe that the values of label smoothing have an impact on the performance, but there is no evident pattern. We need to make appropriate adjustments to its values based on the dataset. For instance, we select 0.8 and 0.5 as the most suitable label smoothing values for the WikiPeople-4 and JF17K-3 datasets, respectively. A smoothing value that is too small or too large may cause performance degradation. A smoothing value that is too large may cause the model to overly believe in the smoothed label distribution, thereby reducing the model’s fitting performance on the training set. A smoothing value that is too small may not effectively prevent the model from overfitting the training data, causing the model to be overconfident in the labels of the training samples.

Effect of Embedding Dimension d . In principle, more semantic knowledge could be captured by having a higher number of dimensions in entity, relation, and qualifiers embeddings. However, as shown in Figure 4(b), there is not a strict proportional relationship between embedding dimensions and the actual performance. After reaching a certain value of embedding dimensions, the accuracy stabilizes. In practice, one chooses the minimum value that achieves stability. For example, for the WikiPeople-4 and JF17K-3 datasets, the embedding dimension d is set at 200.

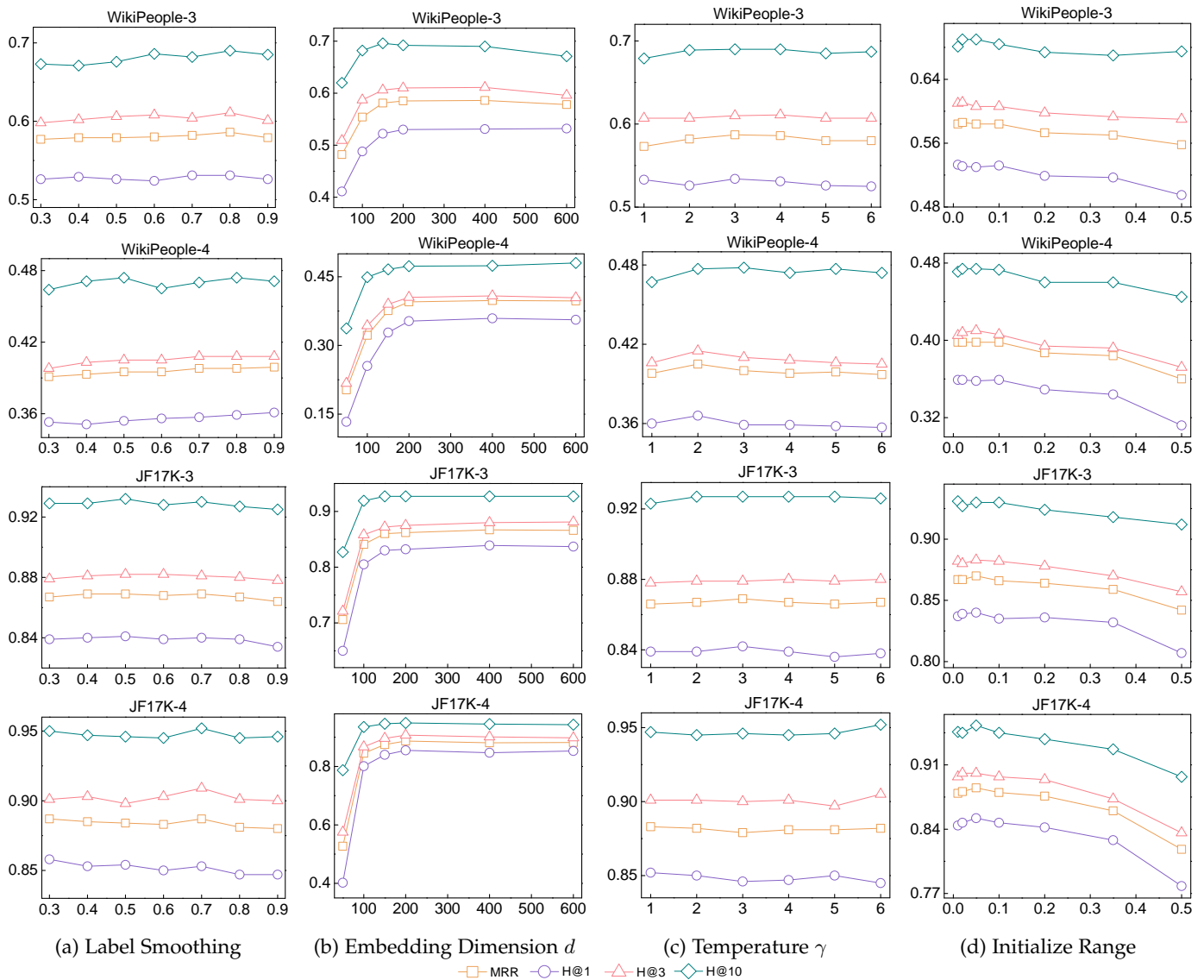


Fig. 4: Parameter sensitivity experiments under different conditions on Wikipeople-3, Wikipeople-4, JF17K-3 and JF17K-4 datasets.

Effect of Temperature γ . The temperature coefficient γ in Equation (1) can be used to adjust the contribution of each neighbor of an entity. Figure 4(c) illustrates the performance difference with values γ ranging from 1 to 6. One can observe that the choice of the γ value has a minimal impact on the final performance. The performance curve only exhibits local oscillations, indicating that the HYPERMONO model is robust to the choice of the γ value.

Effect of the Initialization Range. We observe that the initialization value range of embeddings has a significant impact on HYPERMONO’s performance. As shown in Figure 4(d), when the initialization values are relatively small, the performance of HYPERMONO is more stable. However, the model becomes sensitive to larger initialization values. In practice, it is important to carefully set the initialization range to prevent the model from experiencing sharp performance declines.

5.6 Complexity Analysis

To address **RQ5**, we analyze HYPERMONO’s complexity on the WD50K, WikiPeople, and JF17K datasets from two perspectives: time complexity and space complexity. The corresponding results are shown in Table 8. The time complexity is measured by the number of floating-point operations (#FLOPs) required during training phase, while the space complexity refers to the amount of a model’s parameters (#Params). The larger the values of #FLOPs and #Params are, the more computing power and higher memory usage are required during the training process. We observe that compared with HyperFormer, HYPERMONO requires less time and space overhead in each dataset. Specifically, on the WD50K dataset, HYPERMONO only requires nearly half the #FLOPs and one-sixth the #Params of HyperFormer, which demonstrates that HYPERMONO is more efficient and can achieve better results while occupying less time and space.

TABLE 8: Amount of parameters and calculation of the HyperFormer and HYPERMONO models.

Metrics	Model	WD50K	WikiPeople	JF17K
#FLOPs	HyperFormer	118.397G	118.167G	118.070G
	HYPERMONO	69.600G	69.371G	69.273G
#Params	HyperFormer	66.956M	66.956M	66.956M
	HYPERMONO	10.645M	10.645M	10.645M

6 CONCLUSIONS

In this paper, we propose HYPERMONO, a framework for hyper-relational graph completion that properly implements two-stage reasoning and faithfully captures qualifier monotonicity. Specifically, we model each qualifier as a shrinking of the main triple cone to a qualifier cone to realize qualifier monotonicity. At the same time, we facilitate the integration of coarse-grained inference results derived solely from main triples and fine-grained inference results obtained from hyper-relational facts with qualifiers. Empirical experiments under various settings on the WD50K, WikiPeople, and JF17K datasets demonstrate HYPERMONO’s robust performance, when compared to competitive baselines. Additionally, we present various ablation studies on model transferability, parameter sensitivity, and complexity analysis.

7 FUTURE WORK

As for future work, on the one hand, we believe that it is necessary to pay special attention to numerical attribute knowledge in hyper-relational knowledge. It is unscientific to simply treat numbers as an independent entity. Therefore, we plan to construct a hyper-relational knowledge graph with discrete numbers for further research. On the other hand, there is some readily available schema knowledge for the entities in the knowledge graph. How to elegantly integrate this knowledge into the representation process is also an interesting line of research.

REFERENCES

- [1] A. Bordes, N. Usunier, A. García-Durán, J. Weston, and O. Yakhnenko, “Translating embeddings for modeling multi-relational data,” in *NeurIPS*. Lake Tahoe, Nevada, United States: Curran Associates, 2013, pp. 2787–2795.
- [2] Z. Sun, Z. Deng, J. Nie, and J. Tang, “Rotate: Knowledge graph embedding by relational rotation in complex space,” in *ICLR*. New Orleans, LA, USA: OpenReview.net, 2019, pp. 1–18.
- [3] R. Li, J. Zhao, C. Li, D. He, Y. Wang, Y. Liu, H. Sun, S. Wang, W. Deng, Y. Shen, X. Xie, and Q. Zhang, “House: Knowledge graph embedding with householder parameterization,” in *ICML*. Baltimore, Maryland, USA: PMLR, 2022, pp. 13 209–13 224.
- [4] Z. Zhang, J. Wang, J. Chen, S. Ji, and F. Wu, “Cone: Cone embeddings for multi-hop reasoning over knowledge graphs,” in *NeurIPS*. online: Curran Associates, 2021, pp. 19 172–19 183.
- [5] Z. Hu, V. Gutiérrez-Basulto, Z. Xiang, X. Li, R. Li, and J. Z. Pan, “Type-aware embeddings for multi-hop reasoning over knowledge graphs,” in *IJCAI*. Vienna, Austria: ijcai.org, 2022, pp. 3078–3084.
- [6] C. Nguyen, T. French, W. Liu, and M. Stewart, “Scone: Simplified cone embeddings with symbolic operators for complex logical queries,” in *ACL*. Toronto, Canada: ACL, 2023, pp. 11 931–11 946.
- [7] D. Q. Nguyen, T. Vu, T. D. Nguyen, D. Q. Nguyen, and D. Q. Phung, “A capsule network-based embedding model for knowledge graph completion and search personalization,” in *NAACL*. Minneapolis, the United States: NAACL-HLT, 2019, pp. 2180–2189.
- [8] Y. Gu, T. Zhou, G. Cheng, Z. Li, J. Z. Pan, and Y. Qu, “Relevance search over schema-rich knowledge graphs,” in *WSDM*. Melbourne, Australia: ACM, 2019, pp. 114–122.
- [9] Z. Hu, V. Gutiérrez-Basulto, Z. Xiang, R. Li, and J. Z. Pan, “Transformer-based entity typing in knowledge graphs,” in *EMNLP*. Abu Dhabi, United Arab Emirates: ACL, 2022, pp. 5988–6001.
- [10] Z. Hu, V. Gutiérrez-Basulto, Z. Xiang, X. Li, R. Li, and J. Z. Pan, “Multi-view contrastive learning for entity typing over knowledge graphs,” in *EMNLP*. Singapore: ACL, 2023, pp. 12 950–12 963.
- [11] Y. Yang, C. Huang, L. Xia, and C. Li, “Knowledge graph contrastive learning for recommendation,” in *SIGIR*. Madrid, Spain: ACM, 2022, pp. 1434–1443.
- [12] D. Zou, W. Wei, X. Mao, Z. Wang, M. Qiu, F. Zhu, and X. Cao, “Multi-level cross-view contrastive learning for knowledge-aware recommender system,” in *SIGIR*. Madrid, Spain: ACM, 2022, pp. 1358–1368.
- [13] J. Wen, J. Li, Y. Mao, S. Chen, and R. Zhang, “On the representation and embedding of knowledge bases beyond binary relations,” in *IJCAI*. New York, NY, USA: ijcai.org, 2016, pp. 1300–1307.
- [14] R. Zhang, J. Li, J. Mei, and Y. Mao, “Scalable instance reconstruction in knowledge bases via relatedness affiliated embedding,” in *WWW*. Lyon, France: ACM, 2018, pp. 1185–1194.
- [15] P. Rosso, D. Yang, and P. Cudré-Mauroux, “Beyond triplets: Hyper-relational knowledge graph embedding for link prediction,” in *WWW*. Taipei, China: ACM, 2020, pp. 1885–1896.
- [16] B. Xiong, M. Nayyeri, S. Pan, and S. Staab, “Shrinking embeddings for hyper-relational knowledge graphs,” in *ACL*. Toronto, Canada: ACL, 2023, pp. 13 306–13 320.
- [17] M. Galkin, P. Trivedi, G. Maheshwari, R. Usbeck, and J. Lehmann, “Message passing for hyper-relational knowledge graphs,” in *EMNLP*. online: ACL, 2020, pp. 7346–7359.
- [18] H. Shomer, W. Jin, J. Li, Y. Ma, and J. Tang, “Learning representations for hyper-relational knowledge graphs,” *CoRR*, vol. abs/2208.14322, pp. 1–10, 2022.
- [19] D. Yu and Y. Yang, “Improving hyper-relational knowledge graph completion,” *CoRR*, vol. abs/2104.08167, pp. 1–5, 2021.
- [20] Q. Wang, H. Wang, Y. Lyu, and Y. Zhu, “Link prediction on n-ary relational facts: A graph-based approach,” in *Findings of the ACL*. online: ACL, 2021, pp. 396–407.
- [21] C. Chung, J. Lee, and J. J. Whang, “Representation learning on hyper-relational and numeric knowledge graphs with transformers,” in *KDD*. Long Beach, CA, USA: ACM, 2023, pp. 310–322.
- [22] H. Luo, H. E, Y. Yang, Y. Guo, M. Sun, T. Yao, Z. Tang, K. Wan, M. Song, and W. Lin, “HAHE: hierarchical attention for hyper-relational knowledge graphs in global and local level,” in *ACL*. Toronto, Canada: ACL, 2023, pp. 8095–8107.
- [23] Z. Hu, V. Gutiérrez-Basulto, Z. Xiang, R. Li, and J. Z. Pan, “Hyperformer: Enhancing entity and relation interaction for hyper-relational knowledge graph completion,” in *CIKM*. Birmingham, UK: ACM, 2023, pp. 803–812.
- [24] C. Nguyen, T. French, W. Liu, and M. Stewart, “Cyle: Cylinder embeddings for multi-hop reasoning over knowledge graphs,” in *EACL*. Dubrovnik, Croatia: ACL, 2023, pp. 1728–1743.
- [25] Z. Wang, J. Zhang, J. Feng, and Z. Chen, “Knowledge graph embedding by translating on hyperplanes,” in *AAAI*. Quebec, Canada: AAAI Press, 2014, pp. 1112–1119.
- [26] B. Fatemi, P. Taslakian, D. Vázquez, and D. Poole, “Knowledge hypergraphs: Prediction beyond binary relations,” in *IJCAI*. online: ijcai.org, 2020, pp. 2191–2197.
- [27] T. Trouillon, C. R. Dance, É. Gaussier, J. Welbl, S. Riedel, and G. Bouchard, “Knowledge graph completion via complex tensor factorization,” *J. Mach. Learn. Res.*, vol. 18, pp. 1–38, 2017.
- [28] Y. Liu, Q. Yao, and Y. Li, “Generalizing tensor decomposition for n-ary relational knowledge bases,” in *WWW*. Taipei, China: ACM, 2020, pp. 1104–1114.
- [29] I. Balazevic, C. Allen, and T. M. Hospedales, “Tucker: Tensor factorization for knowledge graph completion,” in *EMNLP*. Hong Kong, China: ACL, 2019, pp. 5184–5193.
- [30] Y. Liu, Q. Yao, and Y. Li, “Role-aware modeling for n-ary relational knowledge bases,” in *WWW*. Ljubljana, Slovenia: ACM, 2021, pp. 2660–2671.
- [31] S. Guan, X. Jin, J. Guo, Y. Wang, and X. Cheng, “Neuinfer: Knowledge inference on n-ary facts,” in *ACL*. online: ACL, 2020, pp. 6141–6151.

- [32] S. Di and L. Chen, "Message function search for knowledge graph embedding," in *WWW*. Austin, TX, USA: ACM, 2023, pp. 2633–2644.
- [33] S. Vashishth, S. Sanyal, V. Nitin, and P. P. Talukdar, "Composition-based multi-relational graph convolutional networks," in *ICLR*. Addis Ababa, Ethiopia: OpenReview.net, 2020, pp. 1–15.
- [34] J. Chen, T. Ma, and C. Xiao, "Fastgcn: Fast learning with graph convolutional networks via importance sampling," in *ICLR*. Vancouver, Canada: OpenReview.net, 2018, pp. 1–15.
- [35] F. Wu, A. H. S. Jr., T. Zhang, C. Fifty, T. Yu, and K. Q. Weinberger, "Simplifying graph convolutional networks," in *ICML*. Long Beach, California, USA: PMLR, 2019, pp. 6861–6871.
- [36] Y. You, T. Chen, Z. Wang, and Y. Shen, "L2-GCN: layer-wise and learned efficient training of graph convolutional networks," in *CVPR*. Seattle, WA, USA: IEEE, 2020, pp. 2124–2132.
- [37] Y. Lu, D. Yang, P. Wang, P. Rosso, and P. Cudre-Mauroux, "Schema-aware hyper-relational knowledge graph embeddings for link prediction," *TKDE*, 2023.
- [38] H. Luo, H. E, L. Tan, G. Zhou, T. Yao, and K. Wan, "DHGE: dual-view hyper-relational knowledge graph embedding for link prediction and entity typing," in *AAAI*. Washington, DC, USA: AAAI Press, 2023, pp. 6467–6474.
- [39] A. Vaswani, N. Shazeer, N. Parmar, J. Uszkoreit, L. Jones, A. N. Gomez, L. Kaiser, and I. Polosukhin, "Attention is all you need," in *NeurIPS*. Long Beach, CA, USA: Curran Associates, 2017, pp. 5998–6008.
- [40] W. Pan, W. Wei, and X. Mao, "Context-aware entity typing in knowledge graphs," in *EMNLP*. online: ACL, 2021, pp. 2240–2250.
- [41] S. Guan, X. Jin, Y. Wang, and X. Cheng, "Link prediction on n-ary relational data," in *WWW*. San Francisco, CA, USA: ACM, 2019, pp. 583–593.
- [42] D. Vrandečić and M. Krötzsch, "Wikidata: a free collaborative knowledge base," *Commun. ACM*, vol. 57, no. 10, pp. 78–85, 2014.
- [43] K. D. Bollacker, C. Evans, P. K. Paritosh, T. Sturge, and J. Taylor, "Freebase: a collaboratively created graph database for structuring human knowledge," in *SIGMOD*. Vancouver, BC, Canada: ACM, 2008, pp. 1247–1250.
- [44] I. Loshchilov and F. Hutter, "Decoupled weight decay regularization," in *ICLR*. New Orleans, LA, USA: OpenReview.net, 2019, pp. 1–11.
- [45] Z. Chen, X. Wang, C. Wang, and J. Li, "Explainable link prediction in knowledge hypergraphs," in *CIKM*. Atlanta, GA, USA: ACM, 2022, pp. 262–271.
- [46] S. Guan, X. Jin, J. Guo, Y. Wang, and X. Cheng, "Link prediction on n-ary relational data based on relatedness evaluation," *TKDE*, vol. 35, pp. 672–685, 2023.
- [47] S. Di, Q. Yao, and L. Chen, "Searching to sparsify tensor decomposition for n-ary relational data," in *WWW*. online: ACM, 2021, pp. 4043–4054.
- [48] C. Wang, X. Wang, Z. Li, Z. Chen, and J. Li, "Hyconve: A novel embedding model for knowledge hypergraph link prediction with convolutional neural networks," in *WWW*. Austin, TX, USA: ACM, 2023, pp. 188–198.
- [49] Z. Li, C. Wang, X. Wang, Z. Chen, and J. Li, "Hje: Joint convolutional representation learning for knowledge hypergraph completion," *TKDE*, 2024.
- [50] S. Yan, Z. Zhang, X. Sun, G. Xu, S. Li, Q. Liu, N. Liu, and S. Wang, "Polygone: Modeling n-ary relational data as gyro-polygons in hyperbolic space," in *AAAI*. online: AAAI Press, 2022, pp. 4308–4317.
- [51] Z. Li, X. Wang, J. Li, W. Guo, and J. Zhao, "Hycube: Efficient knowledge hypergraph 3d circular convolutional embedding," *CoRR*, vol. abs/2402.08961, pp. 1–11, 2024.
- [52] Z. Zhang, J. Cai, Y. Zhang, and J. Wang, "Learning hierarchy-aware knowledge graph embeddings for link prediction," in *AAAI*. New York, NY, USA: AAAI Press, 2020, pp. 3065–3072.
- [53] X. Liu, S. Zhao, K. Su, Y. Cen, J. Qiu, M. Zhang, W. Wu, Y. Dong, and J. Tang, "Mask and reason: Pre-training knowledge graph transformers for complex logical queries," in *KDD*. Washington, DC, USA: ACM, 2022, pp. 1120–1130.
- [54] Y. Liu, Z. Sun, G. Li, and W. Hu, "I know what you do not know: Knowledge graph embedding via co-distillation learning," in *CIKM*. Atlanta, GA, USA: ACM, 2022, pp. 1329–1338.